Articles

Control of Oxo-Molybdenum Reduction and Ionization Potentials by Dithiolate Donors

Matthew E. Helton,[†] Nadine E. Gruhn,[‡] Rebecca L. McNaughton,[†] and Martin L. Kirk*,[†]

Department of Chemistry, The University of New Mexico, Albuquerque, New Mexico 81731-1096, and the Department of Chemistry, The University of Arizona, Tucson, Arizona 85721-0041

Received November 3, 1999

The compounds (L-N_3)MoO(qdt) and (L-N_3)MoO(tdt) [(L-N_3) = hydrotris(3,5-dimethyl-1-pyrazolyl)borate; tdt = toluene-3,4-dithiolate; qdt = quinoxaline-2,3-dithiolate] have been studied by cyclic voltammetry and photoelectron, magnetic circular dichroism, and electronic absorption spectroscopies, and the experimental data have been interpreted in the context of ab initio molecular orbital calculations on a variety of dithiolate dianion ligands. The PES data reveal very substantial differences between (L-N_3)MoO(qdt) and (L-N_3)MoO(tdt) in that the first ionization (originating from the Mo d_{xy} orbital) for (L-N_3)MoO(qdt) is about 0.8 eV to deeper binding energy than that of (L-N_3)MoO(tdt). This stabilizing effect is also reflected in the solution reduction potentials, where (L-N_3)MoO(qdt) is ∼220 mV easier to reduce than (L-N_3)MoO(tdt). A direct correlation between the relative donating ability of a given dithiolate ligand and the reduction potential of the (L-N_3)MoO(dithiolate) complex has been observed, and a linear relationship exists between the calculated Mulliken charge on the S atoms of the dithiolate dianion and the Mo reduction potential. The study confirms previously communicated work (Helton, M. E.; Kirk, M. L. *Inorg. Chem.* **1999**, *38*, 4384−4385) that suggests that *anisotropic* covalency contributions involving only the out-of-plane S orbitals of the coordinated dithiolate control the Mo reduction potential by modulating the effective nuclear charge of the metal, and this has direct relevance to understanding the mechanism of ferricyanide inhibition in sulfite oxidase. Furthermore, these results indicate that partially oxidized pyranopterins may play a role in facilitating electron and/or atom transfer in certain pyranopterin tungsten enzymes which catalyze formal oxygen atom transfer reactions at considerably lower potentials.

Introduction

Determining the electronic structure of metallo-dithiolates is pivotal in developing a detailed understanding of their role in bioinorganic chemistry as well as materials science.[1−6] Numerous metallo-dithiolates have been synthesized and, depending on the choice of the transition metal and dithiolate, reported to possess lumophoric,[7−9] magnetic,[10−12] and conducting[13] properties. Perhaps the most fascinating function of transition metal dithiolates is their ability to catalyze a variety of formal oxygen atom transfer reactions at the active sites of pyranopterin molybdenum[14] and tungsten[15] enzymes. The X-ray structures of many of these enzymes are now known, and they all reveal a common active site feature which consists of at least one pyranopterin ene-1,2-dithiolate bound to high-valent Mo or W.[16−26] It has been hypothesized that the pyranopterin ene-1,2-dithiolate may act to couple the metal into efficient superex-

[†] The University of New Mexico.
[‡] The University of Arizona.

(1) Inscore, F. E.; McNaughton, R. L.; Westcott, B.; Helton, M. E.; Jones, R. M.; Enemark, J. H.; Kirk, M. L. *Inorg. Chem.* **1999**, *38*, 1401−1410.
(2) Helton, M. E.; Kirk, M. L. *Inorg. Chem.* **1999**, *38*, 4384−4385.
(3) Helton, M. E.; Pacheco, A.; McMaster, J.; Enemark, J. H.; Kirk, M. L. *J. Inorg. Biochem.*, in press.
(4) Jones, R. M.; Inscore, F. E.; Hille, R.; Kirk, M. L. *Inorg. Chem.* **1999**, *38*, 4963−4970.
(5) Carducci, M. D.; Brown, C.; Solomon, E. I.; Enemark, J. H. *J. Am. Chem. Soc.* **1994**, *116*, 11856−11868.
(6) Alemany, P.; Hoffmann, R. *J. Am. Chem. Soc.* **1993**, *115*, 8290−8297.
(7) Paw, W.; Cummings, S. D.; Mansour, M. A.; Connick, W. B.; Geiger, D. K.; Eisenberg, R. *Coord. Chem. Rev.* **1998**, *171*, 125−150.
(8) Cummings, S. D.; Eisenberg, R. *Inorg. Chem.* **1995**, *34*, 2007−2014.
(9) Cummings, S. D.; Eisenberg, R. *Inorg. Chem.* **1995**, *34*, 3396−3403.
(10) Kuppusamy, P.; Ramakrishna, B. L.; Manoharan, P. T. *Proc. Indian Acad. Sci.-Chem. Sci.* **1984**, *93*, 977−1001.
(11) Kuppusamy, P.; Manoharan, P. T. *Chem. Phys. Lett.* **1985**, *118*, 159−163.
(12) Fourmigué, M.; Lenoir, C.; Coulon, C.; Guyon, F.; Amaudrut, J. *Inorg. Chem.* **1995**, *34*, 4979−4985.
(13) (a) Veldhuizen, Y. S. J.; Veldman, N.; Spek, A. L.; Faulmann, C.; Haasnoot, J. G.; Reedjik, J. *Inorg. Chem.* **1995**, *34*, 140−147. (b) Brossard, L.; Ribault, M.; Bousseau, M.; Valade, L.; Cassoux, P. *C. R. Acad. Sci. Paris, Ser. 2* **1986**, *302*, 205−210. (c) Kobayashi, A.; Kim, H.; Sasaki, Y.; Kato, R.; Kobayashi, H.; Moriyama, S.; Nishio, Y.; Kajita, K.; Sasaki, W. *Chem. Lett.* **1987**, 1819−1822. (d) Brossard, L.; Hurdequint, H.; Ribault, M.; Valade, L.; Legros, J.-P.; Cassoux, P. *Synth. Met.* **1988**, *27*, B157−B162. (e) Tajima, H.; Inokuchi, M.; Kobayashi, A.; Ohta, T.; Kato, R.; Kobayashi, H.; Kuroda, H. *Chem. Lett.* **1993**, 1235−1238.
(14) Hille, R. *Chem. Rev.* **1996**, *96*, 2757−2816.
(15) Johnson, M. K.; Rees, D. C.; Adams, M. W. W. *Chem. Rev.* **1996**, *96* (6), 2817−2839.
(16) Chan, M. K.; Mukund, S.; Kletzin, A.; Adams, M. W. W.; Rees, D. C. *Science* **1995**, *267*, 1463−1469.
(17) Hu, Y.; Faham, S.; Roy, R.; Adams, M. W. W.; Rees, D. C. *J. Mol. Biol.* **1999**, *286*, 899−914.
(18) Czjzek, M.; Dos Santos, J.-P.; Pommier, J.; Giordano, G.; Mejean, V.; Haser, R. *J. Mol. Biol.* **1998**, *284*, 435−447.
(19) Romão, M. J.; Archer, M.; Moura, I.; Moura, J. J.; LeGall, J.; Engh, R.; Schneider, M.; Hof, P.; Huber, R. *Science* **1995**, *270*, 1170−1176.
(20) Boyington, J. C.; Gladyshev, V. N.; Khangulov, S. V.; Stadtman, T. C.; Sun, P. D. *Science* **1997**, *275*, 1305−1308.

10.1021/ic9912878 CCC: $19.00
Published on Web 05/09/2000

Scheme 1

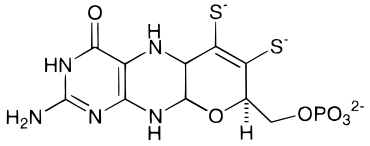

change pathways for facilitating electron-transfer regeneration of the active site,[1] in addition to functioning as a modulator of the metal ion reduction potential (Scheme 1).[2,14] Therefore, the widely varying electronic properties observed in synthetic metallo-dithiolates may be exploited by nature to accomplish multiple tasks at a single active site.

Photoelectron spectroscopy (PES) provides a convenient probe of metal ion effective nuclear charge and the nature of the metal−ligand bond via the energy of valence electron photoionizations. Recently, PES spectroscopy has been employed in the study of oxo-molybdenum compounds of the type (L-N_3)MoE(X,Y) [E = O, S, NO; X, Y = halide, alkoxide, or thiolate; (L-N_3) = hydrotris(3,5-dimethyl-1-pyrazolyl)borate], to evaluate the synergy between the axial (E) and equatorial (X,Y) donors in affecting the ionization energy of the highest occupied molecular orbital (HOMO) localized on the Mo center.[27−29] These studies have conclusively shown that equatorial dithiolate coordination electronically buffers the Mo center in (L-N_3)MoE(tdt) [tdt = toluene-3,4-dithiolate] from the severe electronic perturbations associated with the enormous variation in the π-donor/acceptor properties of E, and it has been proposed that this is a primary role for the pyranopterin ene-1,2-dithiolate chelate during the course of enzymatic catalysis.

There has been considerable interest in how the inherent electronic structure of a thiolate donor can affect and control important properties of transition metal complexes.[30−33] Specifically, we have been trying to understand how simple variations in the donor ability of a coordinated *dithiolate* affect reduction[2,34,35] and ionization potentials of oxo-molybdenum dithiolates. This paper describes the results of a combined spectroscopic study on (L-N_3)MoO(qdt) [qdt = quinoxaline-2,3-dithiolate] and (L-N_3)MoO(tdt), which serve as first-generation models for a variety of pyranopterin Mo enzymes (Scheme 2).[1−5] Photoelectron spectroscopy reveals that the Mo d_{xy} redox orbital of (L-N_3)MoO(qdt) is stabilized ~0.8 eV compared to that of (L-N_3)MoO(tdt). Therefore, different dithiolate ligands can have a marked effect on the reduction and ionization potentials of the metal center by varying the donor ability of the coordinated dithiolate. These new results corroborate and extend the conclusions from our earlier studies on (L-N_3)MoO(qdt) which suggested that an electron-withdrawing effect, induced by an oxidized pyrazine ring, results in highly *anisotropic* covalency contributions to M−S bonding and dramatically affects the valence ionization energy of the oxo-molybdenum HOMO.[2]

Scheme 2

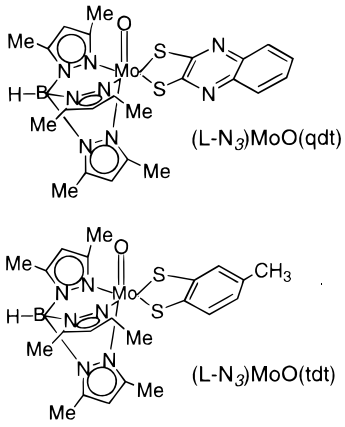

Experimental Section

General Comments. All reactions were carried out in a dinitrogen atmosphere using standard Schlenk techniques, and all solvents were dried, distilled, and deoxygenated prior to use. Purification of solvents was accomplished using the following methodologies: triethylamine from potassium hydroxide; toluene from sodium/benzophenone. Quinoxaline, quinoxaline dichloride, and toluene-3,4-dithiol were purchased from Aldrich, and (L-N_3)$MoOCl_2$,[36] (L-N_3)MoO(tdt),[36] and H_2qdt[8,37] were prepared as previously described.

Abbreviations. Hydrotris(3,5-dimethyl-1-pyrazolyl)borate (L-N_3); ethane-1,2-dithiolate (ead); ethene-1,2-dithiolate (edt); toluene-3,4-dithiolate (tdt); benzene-1,2-dithiolate (bdt); maleonitriledithiolate (mnt); quinoxaline-2,3-dithiolate (qdt); quinoxaline (qn); quinoxaline-1,2-dichloride ($qnCl_2$); quinoxaline-2,3-dithiol [H_2qdt(*ol*)]; quinoxaline-2,3-dithione [H_2qdt(*one*)]; toluene-3,4-dithiol (H_2tdt).

Preparation of (L-N_3)MoO(qdt). A dry toluene solution containing 0.41 g (2.1 mmol) of H_2qdt and 150 μL (2.1 mmol) of triethylamine was added dropwise by cannula at 70 °C to a dry toluene solution of (L-N_3)$MoOCl_2$ (0.5 g, 1.05 mmol). The solution was allowed to react for approximately 13 h, during which time the color of the solution changed from lime green to dark red. The resulting dark red solution was filtered and concentrated under vacuum to precipitate a dark red powder, which was subsequently redissolved in a minimum amount of toluene and chromatographed on silica gel. The compound eluted in a binary mixture of toluene: 1,2-dichloroethane (1:1) as a red band. Yield = 25%. Anal. Calcd for $C_{23}H_{26}N_8OS_2BMo$: C, 45.93; H, 4.36. Found: C, 45.04; H, 4.33. IR (KBr, cm^{-1}): ν(Mo≡O) 940, ν(B−H) 2551. MS (FAB): m/z = 602 (parent ion), 507 (parent − 3,5 dimethylpyrazole), 410 (parent − dithiolate).

Physical Characterization and Electronic Spectroscopy. Elemental analysis was performed at The University of New Mexico using a

(21) Dias, J. M.; Than, M. E.; Humm, A.; Huber, R.; Bourenkov, G. P.; Bartunik, H. D.; Bursakov, S.; Calvete, J.; Caldeira, J.; Carneiro, C.; Moura, J. J. G.; Moura, I.; Romão, M. J. *Structure* **1999**, *7*, 65−79.
(22) Schindelin, H.; Kisker, C.; Hilton, J.; Rajagopalan, K. V.; Rees, D. C. *Science* **1996**, *272*, 1615−1621.
(23) Schneider, F.; Löwe, J.; Huber, R.; Schindelin, H.; Kisker, C.; Knäblein, J. *J. Mol. Biol.* **1996**, *263*, 53−69.
(24) McAlpine, A. S.; McEwan, A. G.; Shaw, A. L.; Bailey, S. *J. Biol. Inorg. Chem.* **1997**, *2*, 690−701.
(25) McAlpine, A. S.; McEwan, A. G.; Bailey, S. *J. Mol. Biol.* **1998**, *275*, 613−623.
(26) Kisker, C.; Schindelin, H.; Pacheco, A.; Wehbi, W. A.; Garrett, R. M.; Rajagopalan, K. V.; Enemark, J. H.; Rees, D. *Cell* **1997**, *91*, 973−983.
(27) Westcott, B. L.; Gruhn, N. E.; Enemark, J. H. *J. Am. Chem. Soc.* **1998**, *120*, 3382−3386.
(28) Westcott, B. L.; Enemark, J. H. *Inorg. Chem.* **1997**, *36*, 5404−5405.
(29) Chang, C. S. J.; Rai-Chaudhuri, A.; Lichtenberger, D. L.; Enemark, J. H. *Polyhedron* **1990**, *9*, 1965−1973.
(30) Sellmann, D.; Hadawi, B.; Knoch, F. *Inorg. Chim. Acta* **1996**, *244*, 213−220.
(31) Sellmann, D.; Mahr, G.; Knoch, F.; Moll, M. *Inorg. Chim. Acta* **1994**, *224*, 35−43.
(32) Musie, G.; Reibenspies, J. H.; Darensbourg, M. Y. *Inorg. Chem.* **1998**, *37*, 302−310.
(33) Izumi, Y.; Glaser, T.; Rose, K.; McMaster, J.; Basu, P.; Enemark, J. H.; Hedman, B.; Hodgson, K. O.; Solomon, E. I. *J. Am. Chem. Soc.* **1999**, *121*, 10035−10046.
(34) Davies, E. S.; Beddoes, R. L.; Collison, D.; Dinsmore, A.; Docrat, A.; Joule, J. A.; Wilson, C. R.; Garner, C. D. *J. Chem. Soc., Dalton Trans.* **1997**, *21*, 3985−3995.
(35) Davies, E. S.; Aston, G. M.; Beddoes, R. L.; Collison, D.; Dinsmore, A.; Docrat, A.; Joule, J. A.; Wilson, C. R.; Garner, C. D. *J. Chem. Soc., Dalton Trans.* **1998**, *21*, 3647−3656.
(36) Cleland, W. E., Jr.; Barnhart, K. M.; Yamanouchi, K.; Collison, D.; Mabbs, F. E.; Ortega, R. B.; Enemark, J. H. *Inorg. Chem.* **1987**, *26*, 1017−1025.

Perkin-Elmer 2400 CHN elemental analyzer equipped with a Perkin-Elmer AD-6 autobalance. Mass spectra were collected at The Nebraska Center for Mass Spectrometry in the Department of Chemistry at the University of Nebraska−Lincoln. Infrared spectra were recorded on a BOMEM MB-100 FT-IR spectrometer as pressed KBr disks.

Low-temperature MCD spectra were collected on a system consisting of a Jasco-J600 CD spectropolarimeter employing Hamamatsu photomultiplier tubes of either S-1 or S-20 response, an Oxford Instruments SM4000-7T superconducting magnetooptical cryostat (0−7 T and 1.4−300 K), and an Oxford Instruments ITC503 temperature controller. The spectrometer was calibrated for CD intensity using camphorsulfonic acid and for wavelength using neodymium-doped glass. Depolarization of the incident radiation was checked by comparing the difference in CD intensity of a standard Ni(+)−tartrate solution positioned in front of and then in back of the sample. Solution electronic absorption spectra were collected on a double-beam Hitachi U-3501 UV−vis−NIR spectrophotometer capable of scanning a wavelength region between 185 and 3200 nm. The solution electronic spectra of (L-N_3)MoO(tdt) and (L-N_3)MoO(qdt) were collected in dichloromethane and 1,2-dichloroethane, respectively.

The photoelectron spectra were collected using an instrument that features a 36 cm radius, 8 cm gap hemispherical analyzer with custom-designed sample cells, as well as detection and control electronics.[38] The argon $^2P_{3/2}$ ionization at 15.759 eV was used as an internal calibration lock of the absolute ionization energy, with the difference between the argon $^2P_{3/2}$ and the methyl iodide $^2E_{1/2}$ ionization (9.538 eV) calibrating the ionization energy scale. During data collection the instrument resolution (measured using the fwhm of the argon $^2P_{3/2}$ peak) was 0.020−0.030 eV. All data are intensity corrected with an experimentally determined instrument analyzer sensitivity function. (L-N_3)MoO(tdt) sublimed between 202 and 218 °C [27] and (L-N_3)MoO(qdt) sublimed between 240 and 270 °C at 10^{-4} Torr (monitored using a "K" type thermocouple which passed through a vacuum feed that directly attached to the cell) with no evidence for decomposition upon heating in the solid or gas phase.

Electrochemical data were collected on an EG&G Instruments, Inc. Princeton Applied Research model 273A potentiostat/galvanostat equipped with an X−Y recorder. The electrochemical cell contained a working (nonrotating) platinum disk electrode, a platinum wire auxiliary electrode, and a Ag/AgCl reference electrode. A 0.1 M tetrabutylammonium hexafluorophosphate solution was utilized as the supporting electrolyte and 2 mM ferrocene as an internal standard.[39] All potentials are reported vs the ferrocene/ferrocenium (Fc/Fc^+) couple (+402 mV) for this electrochemical cell. Cyclic voltammetric measurements were performed on 1,2-dichloroethane solutions of (L-N_3)MoOCl_2, (L-N_3)MoO(qdt), and (L-N_3)MoO(bdt) over a potential range of ±2 V with a scan speed of 100 mV/s. The reduction potentials for (L-N_3)MoO(tdt) and (L-N_3)MoO(ead) have been previously reported.[36]

PES Data Analysis. The vertical length of each data point represents the experimental variance of that point. The valence ionization bands are represented analytically with the best fit of asymmetric Gaussian functions,[40] and the bands are defined by the position, amplitude, half-width for the high binding energy side of the peak, and half-width for the low binding energy side of the peak. The peak positions and half-widths are reproducible to about ±0.02 eV. The number of peaks used in a given fit are based solely on the features of a given band profile. The parameters describing an individual ionization peak are less certain when two or more peaks are close in energy and overlap.

Computational Studies. Ab initio molecular orbital calculations were performed on geometry optimized structures of ead, edt, tdt, bdt, qdt, mnt, qn, $qnCl_2$, H_2tdt, H_2qdt(*ol*), and H_2qdt(*one*) using the Gaussian 98W software package[41] running on a Dell Pentium III 550 MHz workstation. A 6-31G** basis set was employed in all of these calculations.

Scheme 3

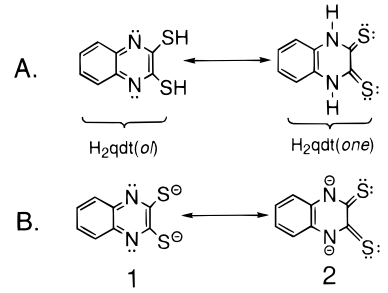

Results and Discussion

Molecular Orbital Calculations. Ab initio quantum chemical calculations were performed on qn, $qnCl_2$, H_2qdt (*ol*), H_2qdt (*one*), H_2tdt, and a variety of additional dithiolate dianions in order to ascertain the nature of their HOMOs. H_2qdt possesses two nearly isoenergetic tautomeric forms, the dithol and dithione, represented in Scheme 3 as H_2qdt (*ol*) and H_2qdt(*one*), respectively. We will use qdt^{2-} to represent the quinoxaline-2,3-dithiolate dianion; however the true ground-state configuration of qdt^{2-} is most likely a quantum mechanical admixture of the two limiting resonance structures in Scheme 3B. The results of the ab initio calculations clearly show that the HOMOs of qn and $qnCl_2$ possess considerable electron density localized in the π^* orbitals of the quinoxaline ring, whereas the electron density of the HOMOs of the dithiolate dianions, including H_2qdt(*ol*) and H_2tdt, is primarily localized on the p orbitals of the sulfur atoms. The dithiolate dianions possess a set of four filled dithiolate sulfur p orbitals, which are energetically isolated from the lower energy bonding MOs predominantly localized on the ring system. These sulfur p orbitals are used in the formation of symmetry-adapted linear combinations with the d orbitals of appropriate symmetry localized on the $[(L\text{-}N_3)MoO]^{2+}$ fragment. Bonding calculations indicate that the ligand frontier valence orbital electron density is largely localized on the sulfur atoms, which is corroborated by experimental results from photoelectron spectroscopy.[42] The results of Mulliken population analyses on the dithiolate dianions provide insight into their relative charge-donating ability, and these results are presented in Figure 1. It is anticipated that as more negative charge is localized on the dithiolate sulfurs, the donor ability of the ligand with respect to a Lewis acid metal will increase. Therefore, $[(L\text{-}N_3)MoO]^{2+}$ fragments coordinated to charge-deficient dithiolates such as qdt^{2-} and mnt^{2-} should be harder to oxidize and possess higher ionization potentials. This results from an increase in

(37) Morrison, D. C.; Furst, A. *J. Org. Chem.* **1956**, *21*, 470−471.
(38) Lichtenberger, D. L.; Kellogg, G. E.; Kristofzski, J. G.; Page, D.; Turner, S.; Klinger, G.; Lorenzen, J. *Rev. Sci. Instrum.* **1986**, *57*, 2366−2366.
(39) Gagne, R. R.; Koval, C. A.; Lisensky, G. C. *Inorg. Chem.* **1980**, *19*, 2854−2855.
(40) Lichtenberger, D. L.; Copenhaver, A. S. *J. Elect. Spec. Relat. Phenom.* **1990**, *50*, 335−352.
(41) Frisch, M. J.; Trucks, G. W.; Schlegel, H. B.; Scuseria, G. E.; Robb, M. A.; Cheeseman, J. R.; Zakrzewski, V. G.; Montgomery Jr., J. A.; Stratmann, R. E.; Burant, J. C.; Dapprich, S.; Millam, J. M.; Daniels, A. D.; Kudin, K. N.; Strain, M. C.; Farkas, O.; Tomasi, J.; Barone, V.; Cossi, M.; Cammi, R.; Mennucci, B.; Pomelli, C.; Adamo, C.; Clifford, S.; Ochterski, J.; Petersson, G. A.; Ayala, P. Y.; Cui, Q.; Morokuma, K.; Malick, D. K.; Rabuck, A. D.; Raghavachari, K.; Foresman, J. B.; Cioslowski, J.; Ortiz, J. V.; Baboul, A. G.; Stefanov, B. B.; Liu, G.; Liashenko, A.; Piskorz, P.; Komaromi, I.; Gomperts, R.; Martin, R. L.; Fox, D. J.; Keith, T.; Al-Laham, M. A.; Peng, C. Y.; Nanayakkara, A.; Gonzalez, C.; Challacombe, M.; Gill, P. M. W.; Johnson, B.; Chen, W.; Wong, M. W.; Andres, J. L.; Gonzalez, C.; Head-Gordon, M.; Replogle, E. S.; Pople, J. A. *Gaussian 98*, Revision A.7; Gaussian, Inc.: Pittsburgh, PA, 1998.
(42) Gleiter, R.; Spanget-Larsen, J. *Top. Curr. Chem.: Spectrosc.* **1979**, *86*, 139−196.

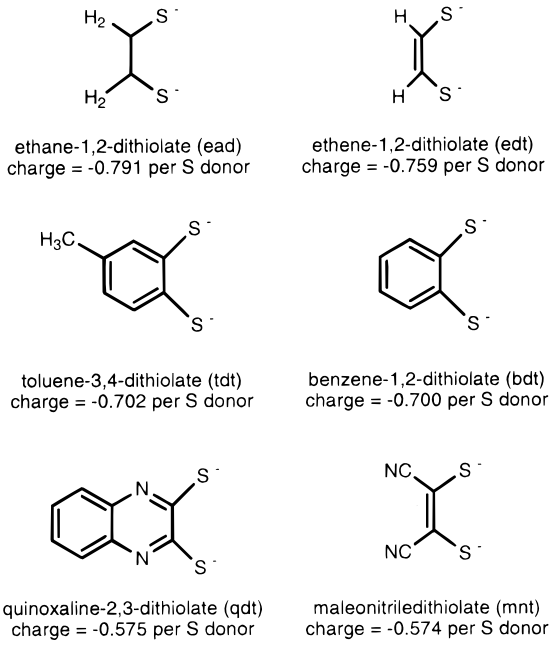

Figure 1. Structures of the dithiolate dianions used in this study. Ab initio molecular orbital calculations were performed on geometry optimized structures, and a 6-31G** basis set was used throughout. The calculated Mulliken charge *per S donor* is listed below each dithiolate.

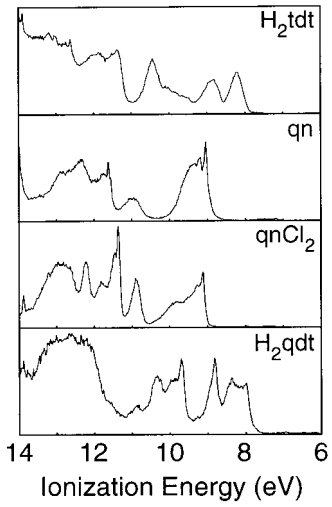

Figure 2. He I photoelectron spectra of H_2tdt, qn, $qnCl_2$, and H_2qdt.

the effective nuclear charge on the metal center brought about by the poor donating ability of these charge-deficient dithiolates.

Ligand PES. The He I PES of H_2tdt, qn, $qnCl_2$, and H_2qdt between 6 and 13 eV are presented in Figure 2. The PES spectra for qn, $qnCl_2$, and H_2qdt reveal similar ionizations in the region between 9 and 11 eV, and these ionizations are assigned as arising from the quinoxaline ring fragment since they are absent in the PES of H_2tdt. This is consistent with the computational results that show that the HOMOs of qn and $qnCl_2$ possess considerable electron density in the quinoxaline π system (vide supra). Ionizations at binding energies less than ~9 eV occur only for H_2qdt and H_2tdt, consistent with their assignment as sulfur-based ionizations. Unexpectedly, the thiol sulfur ionizations for H_2qdt occur at energies similar to those of H_2tdt. Larger differences in ionization potential might have been expected due to an inductive effect caused by the electron-withdrawing pyrazine ring N atoms of H_2qdt and would be consistent with

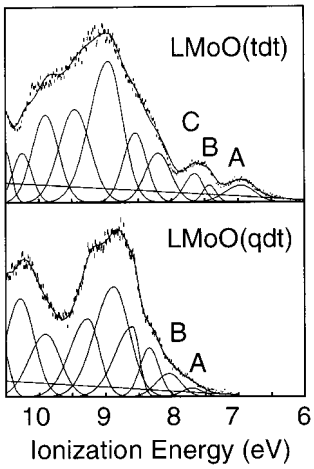

Figure 3. He I photoelectron spectra of (L-N_3)MoO(tdt) (top) and (L-N_3)MoO(qdt) (bottom). Band A is the ionization of the Mo d_{xy} electron, and bands B and C have been assigned as ionizations from the two out-of-plane S_{op} orbitals localized on the ene-1,2-dithiolate. The vertical length of each data point represents the experimental variance of that point, and valence ionization bands are represented analytically with the best fit of asymmetric Gaussian functions. Peak positions and half-widths are reproducible to ±0.02 eV.

Scheme 4

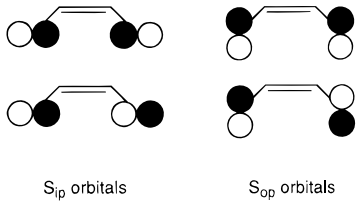

the computed reduction in negative charge on the H_2qdt(*ol*) sulfur (+0.0412) compared with that of H_2tdt (−0.208). The He II photoelectron spectrum of H_2(qdt) shows ionization intensity changes with respect to the He I spectrum. This indicates that ionizations which occur at binding energies less than 9 eV originate from orbitals possessing predominantly sulfur character but also contain carbon and some nitrogen character.[43] This mix of atomic character indicates delocalization between the sulfur and ring π system that is sufficient to destabilize the first ionizations of H_2(qdt) and results in the similar ionization potentials for these protonated dithiolates. Nevertheless, the computed charges on the sulfur atoms of tdt^{2-} and qdt^{2-} indicate that Mo−S covalency will be severely attenuated in metal complexes of qdt^{2-}, resulting in marked effects on the Mo valence ionization energies and reduction potentials.

PES of Oxo-Molybdenum Dithiolates. The 6−11 eV He I PES of the oxo-Mo ene-1,2-dithiolates (L-N_3)MoO(tdt)[27] and (L-N_3)MoO(qdt) are displayed in Figure 3. The general shape of the spectral profile for (L-N_3)MoO(qdt) between 8.5 and 10.5 eV is very similar to that of alkoxide complexes such as (L-N_3)MoO(OEt)$_2$ that have been previously reported.[28,29] The ionizations in this spectral region are primarily associated with the orbitals of the (L-N_3) ligand and the quinoxaline ring of the qdt^{2-} ligand. The spectral differences between (L-N_3)MoO(tdt) and (L-N_3)MoO(qdt) in this region are due to the presence of the tolyl π ionizations at ~9.5 eV in the spectrum of (L-N_3)-MoO(tdt). However, the most striking differences between (L-N_3)MoO(tdt) and (L-N_3)MoO(qdt) occur in the region below

(43) Glass, R. S.; Broeker, J. L.; Jatcko, M. E. *Tetrahedron* **1989**, *45*, 1263−1272.

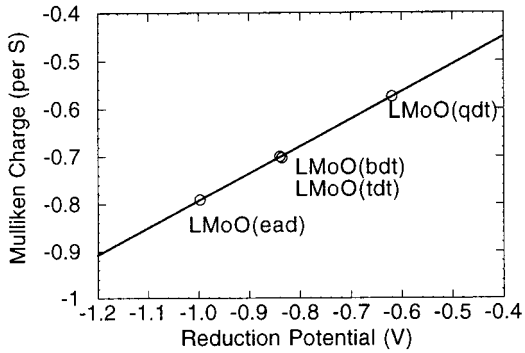

Figure 4. Plot of the reduction potential for (L-N_3)MoO(ead), (L-N_3)-MoO(bdt), (L-N_3)MoO(tdt), and (L-N_3)MoO(qdt) as a function of calculated Mulliken charge per S atom of the respective dithiolate dianion. The reference electrode was Ag/AgCl, and the Mo(V)/Mo-(IV) reduction potentials are reported here vs a Fc/Fc^+ internal standard.[44] (L-N_3)MoO(ead) = −0.997 V, (L-N_3)MoO(tdt) = −0.836 V, (L-N_3)MoO(bdt) = −0.840 V, and (L-N_3)MoO(qdt) = −0.620 V. The Mo(V)/Mo(IV) wave observed in the cyclic voltammetry of these compounds is quasi-reversible, with a ΔE close to the theoretical value of 0.0592.

Table 1. Comparison of the Fit Data for (L-N_3)MoO(qdt) and (L-N_3)MoO(tdt)

compound	band	position (eV)	half-width (eV) high	half-width (eV) low	relative area
(L-N_3)MoO(qdt)	A	7.72	0.34	0.34	1.00
	B	8.04	0.46	0.42	3.29
(L-N_3)MoO(tdt)	A	6.95	0.56	0.47	1.00
	B	7.43	0.23	0.23	0.45
	C	7.65	0.36	0.30	2.40

8.5 eV. For (L-N_3)MoO(tdt), there are two ionization bands between 6 and 8 eV that are energetically isolated from the other ligand-based ionizations. Since the Mo ion in these complexes is in the +5 oxidation state (d^1), band A of (L-N_3)MoO(tdt) (Figure 3) has been attributed to the ionization of this Mo valence electron.[27,28] The valence ionization energy of the d_{xy} orbital in oxo-molybdenum dithiolates is of considerable interest since it is the active orbital in metal-centered redox processes. The d_{xy} orbital contains a large amount of sulfur character resulting from orbital mixing with the in-plane sulfur p orbitals (S_{ip}) of the tdt ligand (Scheme 4).[1,27] The second band, which has been fit with two Gaussians (B and C in Figure 3), is associated with ionizations from the symmetric and antisymmetric combinations of out-of-plane sulfur p orbitals (S_{op}) on the tdt^{2-} ligand. In contrast, the d_{xy} and S_{op} orbitals of (L-N_3)-MoO(qdt) are considerably stabilized with respect to (L-N_3)-MoO(tdt) such that they are partially obscured by the (L-N_3) ligand and quinoxaline ring ionizations (Figure 3, bottom panel). These ionizations can be observed as a sloping shoulder on the low-energy side of the ligand ring ionizations and can be fit with two Gaussian bands labeled A and B. The position of band A has been stabilized by ∼0.77 eV from the first ionization energy of (L-N_3)MoO(tdt), revealing the dramatic influence of different dithiolates on the valence ionization energy of the d_{xy} redox orbital. A comparison of the best fits to the PES data for (L-N_3)MoO(tdt) and (L-N_3)MoO(qdt) are presented in Table 1.

Electrochemistry. The reduction potential for (L-N_3)MoO-(qdt), together with previously reported data for other (L-N_3)-MoO(dithiolate) complexes,[36] is presented graphically as a function of the *dithiolate ligand* Mulliken charge in Figure 4. It is readily apparent that a linear relationship exists between the solution reduction potentials and the calculated Mulliken charge per S atom for the four dithiolate dianions, ead^{2-}, tdt^{2-}, bdt^{2-}, and qdt^{2-}. The straight line represents the best fit to the data, and the equation describing this relationship is given below:

$$E_{red} = 1.754 \times \text{charge} + 0.386$$

Note that the more negative the charge localized on sulfur for a given dithiolate donor, the more difficult the corresponding (L-N_3)MoO(dithiolate) complex is to reduce. Thus, the Mulliken charge calculated for a dithiolate S donor is an *excellent* predictor of the solution reduction potential. Furthermore, a linear relationship has also been found to exist between the reduction and ionization potentials in the (L-N_3)MoE$(OR)_2$ series,[29] and it can be inferred that the calculated charge localized on the sulfur donors will be an excellent predictor of this property as well. Summarizing, the electrochemical results are consistent with the PES data and indicate that there is an increase in the effective nuclear charge on Mo in (L-N_3)MoO-(qdt). This increase in effective nuclear charge is a direct function of the reduced negative charge localized on the qdt sulfur atoms (Figure 1), resulting in qdt^{2-} being a poorer donor to Mo when compared to other electron-rich dithiolates.

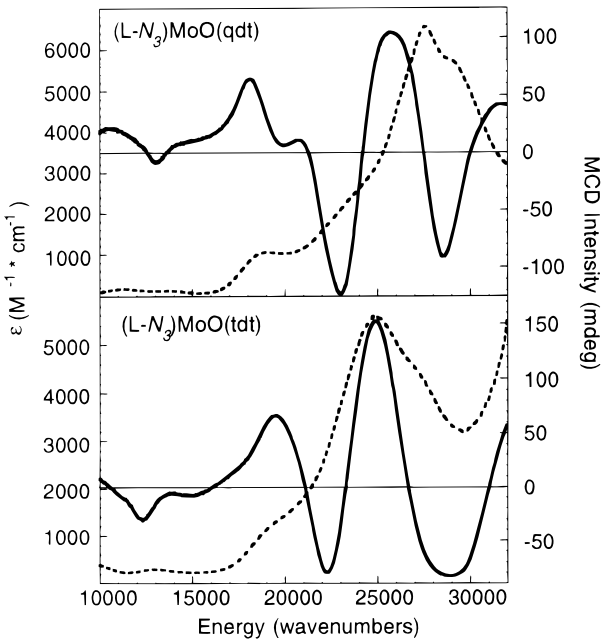

Figure 5. Room-temperature electronic absorption spectra (dashed line) and 5 K, 7 T MCD spectra (solid line) of (L-N_3)MoO(qdt) (top) and (L-N_3)MoO(tdt) (bottom).

Electronic Absorption and MCD Spectroscopy. Electronic spectroscopies can be used to probe the precise orbital contributions to the observed differences in ionization and reduction potentials at higher resolution. The 298 K solution absorption and 5 K, 7 T mull MCD spectra of (L-N_3)MoO(tdt) and (L-N_3)MoO(qdt) are given in Figure 5. We have recently undertaken an extensive electronic structure study of oxo-molybdenum dithiolates and have assigned all of the S → Mo CT bands in (L-N_3)MoO(bdt)[1] and (L-N_3)MoO(tdt)[1,5] which occur at energies below ∼26 000 cm^{-1}. The close correspondence in MCD spectral features observed for (L-N_3)MoO(qdt) and (L-N_3)MoO-(tdt) results in the same band assignments being transferred to (L-N_3)MoO(qdt). The intensity of the S_{ip} → Mo d_{xy} transition probes the dominant covalency contributions between the Mo

Table 2. Transition Energies and Molar Extinction Coefficients for the S → Mo CT Bands of (L-N_3)MoO(tdt) and (L-N_3)MoO(qdt)

	(L-N_3)MoO(tdt)		(L-N_3)MoO(qdt)	
	energy (cm^{-1})	ϵ (M^{-1} cm^{-1})	energy (cm^{-1})	ϵ (M^{-1} cm^{-1})
S_{op} → Mo d_{xy}	9070	490	11 267	174
S_{op} → Mo d_{xy}	13 030	274	13 717	133
S_{ip} → Mo d_{xy}	19 624	1324	19 085	1050
S_{op} → Mo $d_{xz}d_{yz}$	24 761	5491	25 670	4027

d_{xy} redox orbital and the dithiolate S_{ip} orbitals.[1,45] The transition energies and molar extinction coefficients for (L-N_3)MoO(tdt) and (L-N_3)MoO(qdt) are presented in Table 2 for comparative purposes. The similar S_{ip} → Mo d_{xy} charge-transfer intensity between (L-N_3)MoO(tdt) and (L-N_3)MoO(qdt) reflects nearly equivalent pseudo-σ-mediated charge donation (covalency) between the in-plane orbitals of the two ene-1,2-dithiolates and the oxo-molybdenum d_{xy} orbital. Since the nature of the in-plane bonding interaction is essentially equivalent in (L-N_3)-MoO(tdt) and (L-N_3)MoO(qdt), this can not be the origin of the marked differences in the reduction and ionization potential between these two complexes. Interestingly, the electronic absorption spectra reveal that the S_{op} → Mo $d_{xz,yz}$ transition for (L-N_3)MoO(tdt) is much more intense than those observed for (L-N_3)MoO(qdt). The observed differences in S_{op} → Mo $d_{xz,yz}$ charge-transfer intensity reflect a substantial change in the nature of Mo-dithiolate bonding between these complexes, and we attribute this to the greater S_{op} donor ability of the tdt^{2-} ligand relative to qdt^{2-}. Therefore, the large differences observed in the reduction and ionization potentials result from a highly *anisotropic* bonding scheme, whereby the S_{op} donor ability of the qdt^{2-} ligand is severely compromised relative to tdt^{2-}, resulting in an increase in the effective nuclear charge on Mo in (L-N_3)MoO(qdt).

Conclusions

The combined spectroscopic, electrochemical, and computational results presented here support the conclusion that oxo-Mo reduction potentials can be dramatically influenced by the nature of the dithiolate bound to the metal center, and the origin of this behavior lies in dithiolate-dependent differences in Mo−S covalency. Thus, these results provide deeper insight into the nature of metal−dithiolate bonding interactions, in particular those relevant to the mechanism of pyranopterin Mo and W enzymes. Previous PES studies have shown that tdt^{2-} possesses the remarkable ability to poise the Mo center at nearly constant ionization potential (ΔE_{ip} = 0.07 eV) in the (L-N_3)MoE(tdt) series.[27] However, when the dithiolate ligand is replaced by alkoxide donors, the ionization potential of (L-N_3)MoO$(OR)_2$ is ∼0.9 eV easier to ionize than (L-N_3)Mo(NO)$(OR)_2$. This "electronic buffer" effect[27] has been suggested to be a general property of dithiolate donors, and it has been hypothesized that a primary role of the pyranopterin ene-1,2-dithiolate in molybdenum enzymes is to maintain a nearly constant effective nuclear charge on Mo during the course of catalysis. The new results presented here indicate that the qdt^{2-} ligand possesses considerable contributions from the dithione resonance structure (Scheme 3, B2), limiting the ability of the qdt^{2-} sulfur atoms to donate charge to Mo in (L-N_3)MoO(qdt). As a result, we suggest that the electronic buffer effect may be considerably reduced in charge-deficient dithiolates such as qdt^{2-}.

It has been shown that incubation of active sulfite oxidase with ferricyanide results in the two-electron oxidation of the pyranopterin, forming a fully oxidized pyrazine ring fused to a pyran ring that anchors to the Mo ion via an ene-1,2-dithiolate chelate.[46] The electronic effects of the pyrazine ring on Mo in sulfite oxidase is mimicked in (L-N_3)MoO(qdt). Although the ferricyanide-treated enzyme is still competent to oxidize the sulfite substrate, electron transfer from the reduced Mo active site is severely attenuated. Previously, we communicated that the inhibition of electron transfer in ferricyanide-treated sulfite oxidase was likely due to a decrease in the π-donor ability of the oxidized pyranopterin dithiolate.[2] Thus, an increase in the effective nuclear charge on Mo results in a positive shift in the reduction potential, with a concomitant stabilization of the reduced Mo(IV) active site to one-electron oxidation. This hypothesis is supported by the PES data on (L-N_3)MoO(tdt) and (L-N_3)MoO(qdt), which show that electron-deficient dithiolates can stabilize the d_{xy} redox orbital by nearly 1 eV. Finally, it is interesting to speculate whether partially oxidized pyranopterins may play a role in facilitating electron and/or atom transfer in certain pyranopterin tungsten enzymes that catalyze formal oxygen atom transfer reactions at considerably lower potentials.

Acknowledgment. The authors would like to thank Prof. John Enemark for helpful discussions and Frank E. Inscore for use of his (L-N_3)MoO(tdt) data. M.L.K. would like to thank the National Institutes of Health for financial support of this work (Grant No. GM-057378).

IC9912878

(44) The reduction potentials for (L-N_3)MoO(ead) and (L-N_3)MoO(tdt) were taken from ref 30. These potentials were originally referenced vs Ag/AgCl and are reported here vs the ferrocene/ferrocenium couple.

(45) The intensity (I) of a charge-transfer transition is proportional to the square of the overlap integral $\langle\varphi_M|\varphi_L\rangle^2$. See, for example: Solomon, E. I. *Comm. Inorg. Chem.* **1984**, *3*, 225−320.

(46) Gardlik, S.; Rajagopalan, K. V. *J. Biol. Chem.* **1991**, *266*, 4889−4895.